

DCMS: Motion Forecasting with Dual Consistency and Multi-Pseudo-Target Supervision

Maosheng Ye^{1*}, Jiamiao Xu², Xunnong Xu², Tengfei Wang¹, Tongyi Cao²,
Qifeng Chen¹

¹The Hong Kong University of Science and Technology ²DeepRoute.AI

Abstract. We present a novel framework for motion forecasting with Dual Consistency Constraints and Multi-Pseudo-Target supervision. The motion forecasting task predicts future trajectories of vehicles by incorporating spatial and temporal information from the past. A key design of DCMS is the proposed Dual Consistency Constraints that regularize the predicted trajectories under spatial and temporal perturbation during the training stage. In addition, we design a novel self-ensembling scheme to obtain accurate pseudo targets to model the multi-modality in motion forecasting through supervision with multiple targets explicitly, namely Multi-Pseudo-Target supervision. Our experimental results on the Argoverse motion forecasting benchmark show that DCMS significantly outperforms the state-of-the-art methods, achieving 1st place on the leaderboard. We also demonstrate that our proposed strategies can be incorporated into other motion forecasting approaches as general training schemes.

Keywords: Motion Forecasting, Autonomous Driving

1 Introduction

Motion forecasting has been a crucial task for self-driving vehicles to predict the future trajectories of agents (cars, pedestrians) involved in the traffic. Solving this task can help self-driving vehicles to plan their future actions and prevent potential accidents. Motion forecasting is an intrinsically multi-modal problem with substantial uncertainties as the future is not deterministic, implying that an ideal motion forecasting method should produce a distribution of future trajectories or at least multiple most likely future trajectories.

Due to the inherent uncertainty of motion forecasting, this task remains challenging and unsolved yet. Recently, researchers have proposed different architectures based on various representations to encode the kinematic states and context information from HDMap in order to generate feasible multi-modal trajectories [2, 7, 14, 16, 27, 28, 34, 47, 51, 53, 55]. These methods follow a traditional static training pipeline, where each scenario that consists of multiple frames is split

* Work done during an internship at DeepRoute.AI.

into historical data (input) and future data (ground truth) in a fixed pattern. Nevertheless, the prediction task is a streaming task in real-world applications, where the current state will become a historical state as time goes by. The buffer of the historical state is more likely a queue structure to make successive predicted trajectories. As a result, temporal consistency should become a crucial requirement for the downstream tasks for fault and noise tolerance. In traditional planning algorithms [11], trajectory stitching is proposed to ensure stability along the temporal horizon.

Inspired by these phenomena, we raise a question: can we enforce the temporal consistency in the training stage? Naturally, the generated trajectories should be consistent given the successive input along the temporal horizon, namely temporal consistency. Meanwhile, the generated trajectories should be stable and robust enough against small spatial noise or disturbance, and thus spatial consistency should also be considered. Both spatial and temporal consistency can be modeled as self-supervision. We therefore propose our framework **DCMS** in this work, which introduces the consistency constraints in both spatial and temporal domains, namely Dual Consistency Constraints for developing invariant representations.

Apart from that, multi-modality is another core characteristic of the prediction task. Existing datasets [8,45] only provide a single ground-truth trajectory for each scenario, which can not satisfy the multi-choice situations such as junction scenarios. Most methods adopt the winner-takes-all (WTA) [25] or its variants [3,33] to alleviate this situation. Our method addresses this issue directly by introducing more powerful pseudo targets from self-ensembling. With supervision from multiple soft pseudo targets, our model is more likely to be exposed to more high-quality samples, bootstrapping each modality.

Our contributions are summarized as follows.

- We propose Dual Consistency Constraints to enforce temporal and spatial consistency in our model, which is shown to be a general and effective way to improve the overall performance in motion forecasting.
- We propose a self-ensembling-based Multi-Pseudo-Target training strategy that provides multi-modality supervision explicitly during training.
- We conduct extensive experiments on the Argoverse [8] motion forecasting benchmark and the results show that our proposed approach outperforms the state-of-the-art methods in motion forecasting.

2 Related Work

Motion Forecasting. Traditional methods [20,41,50,58] for motion forecasting mainly utilize HDMap information for the prior estimation and Kalman filter [21] for motion states prediction. With the recent progress of deep learning on big data, more and more works have been proposed to exploit the potential of data mining in motion forecasting. Methods [2,7,10,14,19,27,28,42,43,51,53] explore different representations, including rasterized image, graph representation, point cloud representation and transformer to generate the features for the task and

predict the final output trajectories by regression or post-processing sampling. Most of these works focus on finding more effective and compact ways of feature extraction on the surrounding environment (HDMap information) and agent interactions. Based on these representations, other approaches [6,31,43,53,54,55] try to incorporate the prior knowledge with traditional methods, which take the predefined candidate trajectories from sampling or clustering strategies as anchor trajectories. To some extent, these candidate trajectories can provide better guidance and goal coverage for the trajectories regression due to straightforward HDMap encoding. Nevertheless, this extra dependency makes the stability of models highly related to the quality of the trajectory proposals. Goal-guided approaches [15,16] are therefore introduced to optimize goals in an end-to-end manner, paired with sampling strategies that generate the final trajectory for better coverage rate.

Consistency Regularization. Consistency Regularization has been fully studied in semi-supervised and self-supervised learning. Temporally related works [49,26,57] have widely explored the idea for a cyclic consistency. Most of the works apply pairwise matching to minimize the alignment difference through optical flow or correspondence matching to achieve temporal smoothness. Other works [1,13,36,40,48] apply consistency constraints to predictions from the same input with different transformations in order to obtain perturbation-invariant representations. Our work can be seen as a combination of both types of consistency to fully consider the spatial and temporal continuity in motion forecasting.

Multi-hypothesis Learning. Motion forecasting task inherently has multi-modality due to the future uncertainties and difficulties in acquiring accurate ground-truth labels. WTA [17,44] in multi-choice learning and its variants [30,39] incorporate with better distribution estimation to improve the training convergence, thus allowing more multi-modality. Some anchor-based methods [3,7,37,53] introduce pre-defined anchors based on kinematics or road graph topology to provide guidance. However, these methods only allow one target per training stage. Other methods [3,16] try to generate multi-target for supervision with heavy handcrafted optimizations. We propose a Multi-Pseudo-Targets approach to provide more precise trajectory pseudo labels by leveraging the power of self-ensembling [24,56]. Multiple targets are explicitly provided to each agent to better model the multi-modality.

3 Approach

The overall architecture of DCMS consists of three parts. 1) We first utilize a joint spatial and temporal learning framework TPCN [51] to extract point-wise features. Based on these features, we decouple the trajectory prediction problem as a two-stage regression task. The first stage performs goal prediction and completes the trajectory with the goal position guidance. The second stage takes the output of the first stage as anchor trajectories for refinement. 2) To train our DCMS, we propose **Dual Consistency Constraints** to regularize the predictions both spatially and temporally in a streaming task view. 3)

We generate more accurate pseudo labels by self-ensembling to provide **Multi-Pseudo-Target supervision** in Sec. 3.3.

3.1 Architecture

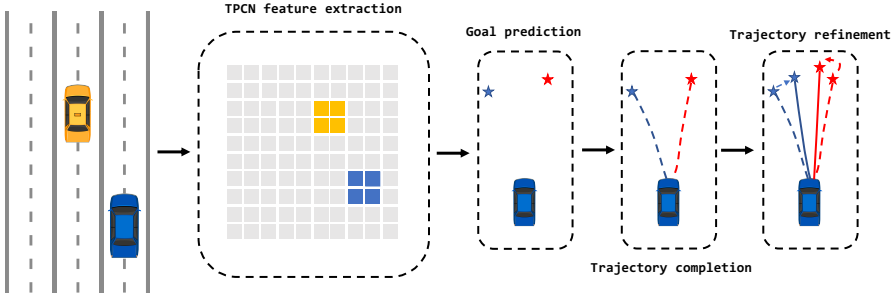


Fig. 1. The overall network structure. We utilize TPCN as a feature extraction backbone to model the spatial and temporal relationship among agents and map information. Then a goal prediction header is used to regress the possible goal candidates; with the goal position, we apply trajectory completion to obtain full trajectories; finally, the trajectories are refined based on the output of the trajectory completion module as anchor trajectories

Recently, TPCN [51] has gained popularity in this task due to its flexibility for joint spatial-temporal learning compared with graph neural networks [27,53] and scalability to adopt more techniques from point cloud learning. Considering its inferiority in representing future uncertainty, we extend TPCN with a two-stage manner through goal position prediction for more accurate waypoints prediction as our baseline. The whole network is shown in Fig. 1.

Feature Extraction: First, TPCN is used as an effective backbone for feature extraction. It utilizes dual-representation point cloud learning techniques with multi-interval temporal learning to model the spatial and temporal relationship. All the historical trajectories of input agents and map information are based on pointwise representation $\{\mathbf{p}_1, \mathbf{p}_2, \dots, \mathbf{p}_N\}$, where \mathbf{p}_i is the i -th point with N points in total, and then go through multi-representation learning framework to generate pointwise features $\mathcal{P} \in R^{N \times C}$, where C is the channel number.

Goal Prediction: With the pointwise features from the backbone, we also adopt the popular goal-based ideas [15,16,55] to find the optimal planning policy. Specifically, we first gather all corresponding pointwise agent features and then sum over features to get the agent instance feature $\phi \in R^{1 \times C}$. To generate K

goal position prediction $G = \{G^k : (g_x^k, g_y^k) | 1 \leq k \leq K\}$, we use a simple MLP layer : $G = MLP(\phi)$.

Compared with previous goal-based methods, we do not rely on heavy sampling strategies and generate too many goal proposals, leading to a large computation overhead.

Trajectory Completion: With the predicted goal positions, we need to complete each trajectory conditioned on these goals. We propose a simple trajectory completion module to generate K full trajectories $\{\tau_{reg}^k | 1 \leq k \leq K\}$ with a single MLP layer as follows:

$$\tau_{reg}^k = \{(x_1^k, y_1^k), (x_2^k, y_2^k), \dots, (x_T^k, y_T^k)\} = MLP(concat(\phi, G^k)). \quad (1)$$

Trajectory Refinement: Inspired by Faster-RCNN [38] and Cascade-RCNN [4], we use the output trajectories from the Trajectory Completion Module as anchor trajectories to refine trajectories and predict the corresponding possibility of each trajectory. In particular, the input of the trajectory refinement module will be the whole trajectory with agent historical waypoints $\tau_{history}$. With a residual block followed by a linear layer Reg and Cls respectively, we regress the delta offset to the first stage outputs $\Delta_{\tau_{reg}}$ and corresponding scores $\tau_{cls} = \{c^k | 1 \leq k \leq K\}$ respectively:

$$\Delta_{\tau_{reg}} = Reg(\tau_{reg}, \tau_{history}), \quad (2)$$

$$\tau_{cls} = Cls(\tau_{reg}, \tau_{history}). \quad (3)$$

The final output trajectories will be $\tau_{reg'} = \Delta_{\tau_{reg}} + \tau_{reg}$.

3.2 Dual Consistency Constraints

Consistency regularization has been proved as an effective self-constraint that helps improve robustness against disturbances. Therefore, we propose **Dual Consistency Constraints** in both spatial and temporal domains to align predicted trajectories for continuity and stability.

Temporal Consistency In motion forecasting, since each training scenario contains multiple successive frames within a fixed temporal chunk, it is reasonable to assume that any two overlapping chunks of input data with a small time-shift should produce consistent results.

A general motion forecasting task aims to predict K possible trajectories with T time steps for one scenario, given M frames historical information. Suppose the information at each history frame is I_i , where $1 \leq i \leq M$ and the k -th output future trajectories are $\{(x_i^k, y_i^k) | M < i \leq M + T\}$. We first apply time step shift s for the input for the temporal consistency. Therefore, the input history frames information will be $\{I_i | 1 + s \leq i \leq M + s\}$ and then we apply the same network for the shifted history information with surrounding HDMap information to

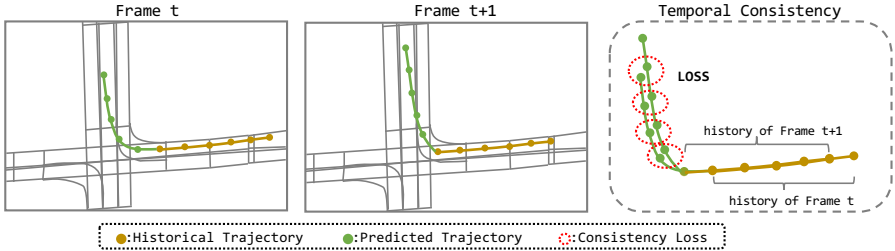


Fig. 2. The overall idea of the temporal consistency. In the training stage, we first generate output prediction trajectory points as normal for each given scenario. Then we slide the input with a step in order to introduce the streaming nature to generate the consecutive output trajectory points. The proposed temporal consistency requires the overlap between these two outputs to be consistent

generate the k -th output trajectories $\{(x_i'^k, y_i'^k) | M + s < i \leq M + s + T\}$. When s is small, the driving intentions or behavior keeps stable in a short period. Since both trajectories have $T - s$ overlapping waypoints, they should be as close as possible and share consensus when s is small. Thus, we can construct self-constraints for a single scenario input due to the streaming property of the input data. Fig. 2 demonstrates the overall idea of the temporal consistency constraint.

Trajectory Matching: Since we predict K future trajectories to deal with the multi-modality, it is crucial to consider the trajectory matching relationship between original predictions and time-shifted predictions when applying the temporal consistency alignment. For a matching problem, the metric on similarity criteria and matching strategies will be two key factors. Several ways can be used to measure the difference between trajectories, such as Average Displacement Error (**ADE**) and Final Displacement Error (**FDE**). We utilize **FDE** as the criteria since the last position error can partially reflect the similarity with less bias from averaging compared with **ADE**.

Matching Strategy: There are roughly four ways used for matching, namely forward matching, backward matching, bidirectional matching, and Hungarian matching. Forward matching takes one trajectory in the current frame and finds its corresponding trajectory in the next frame with the least cost or maximum similarity. Backward matching is the reverse way compared to forward matching. Furtherly, bidirectional matching consists of both forward and backward matching, which considers the dual relationship. Hungarian matching is a linear optimal matching solution based on linear assignment. Forward and backward matching only consider the one-way situation, which is sensitive to noise and unstable. Hungarian matching has a high requirement for cost function choice. Based on these observations, we choose bidirectional matching as our strategy. We also show its advantages over the other approaches in Sec. 4.3.

After obtaining the optimal matching pairs $\{(m_k, n_k) | 1 \leq k \leq K\}$, we can compute the consistency constraint by a simple smooth L_1 loss [38] \mathcal{L}_{Huber} :

$$\mathcal{L}_{temp} = \sum_{k=1}^K \sum_{t=s+1}^T \mathcal{L}_{Huber}((x_t^{m_k}, y_t^{m_k}), (x'_{t-s}^{n_k}, y'_{t-s}^{n_k})). \quad (4)$$

Spatial Consistency Since our DCMS is a two-stage framework, the second stage mainly aims for trajectory refinement. It will be more convenient to add spatial permutation in the second stage with less computational cost. First, we apply spatial permutation function Z , including flipping and random noise, to the trajectories from the first stage. The refinement module will process these augmented inputs and generate the offset to the ground truth and classification scores. Under the small spatial permutation and disturbance, we assume that the outputs of the network should also be self-consistent, meaning that the outputs have strong stability or tolerance to noise.

Since we process the input sequence by sequence in the trajectory refinement module, we do not need to care about the matching problem. It is exactly a one-on-one matching problem. Therefore, spatial consistency is more like an inner-input problem, while temporal consistency is an intra-input problem. Then the spatial consistency constraint \mathcal{L}_{spa} is as follows:

$$\mathcal{L}_{spa} = \mathcal{L}_{Huber}(\Delta_{\tau_{reg}}, Z^{-1}(Reg(Z(\tau_{reg}, \tau_{history}))). \quad (5)$$

Then the total loss for Dual Consistency Constraints module will be $\mathcal{L}_{cons} = \mathcal{L}_{spa} + \mathcal{L}_{temp}$.

3.3 Multi-Pseudo-Target Supervision

Existing datasets [8,45] only provide a single ground-truth trajectory for the target agent, which is to be predicted in one scenario. In order to encourage the multi-modality of models, the winner-takes-all (WTA) strategy is commonly used to avoid model collapsing into a single domain. However, the WTA training strategy suffers from instability associated with network initialization. Some other approaches [3,33] introduce robust estimation methods to select better hypotheses. To some extent, these methods can only implicitly model the multi-modality. Some other approaches [3,55] generate several possible future trajectories based on the kinematics model and road graph topology. DenseTNT [16] only uses pseudo labels for goal set prediction through a hill-climbing algorithm. These optimization methods tend to impose strict constraints and handcrafted prior knowledge, resulting in inaccurate pseudo targets and inferior performance. In contrast, our approach aims to generate more accurate pseudo targets to provide explicit multi-modality supervision through self-ensembling to leverage the power from semi-supervised learning [46,52,56].

Pseudo-Target Generation: The key part of our approach lies in generating more accurate pseudo labels for each agent. It sounds like a “chicken and egg” problem since we need Pseudo-Target to improve the performance. However, it is straightforward to apply model ensembling techniques [18,23,46] to obtain

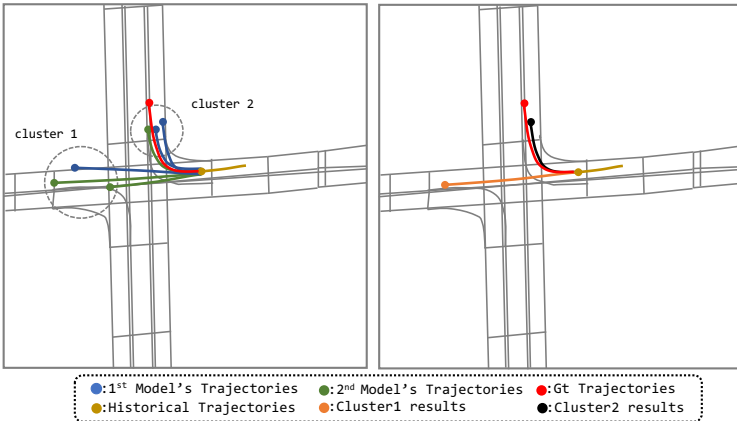


Fig. 3. The overall procedure for the pseudo-target generation. We obtain multiple predictions from outputs of different models for the target agents in each scenario; then we apply k-means clustering algorithm to ensemble the trajectories

more powerful predictions. Compared with previous works [3,7,55], we do not rely on handcrafted anchor trajectory sampling, which is based on inaccurate prior knowledge, including motion estimation. Meanwhile, soft targets from ensembling can better finetune the predictions and reduce the gradient variance for better training convergence. As suggested in works [9,35], the prediction error decreases when the ensemble approach is used once the model is diverse enough. Therefore, we apply k-means algorithm [29] to the predicted trajectories that are collected within different training procedures (for example, launched with different seeds of random number generators, optimized with different learning rates, etc.) of DCMS without Multi-Pseudo-Target supervision to generate J trajectories with corresponding scores for each scenario. Fig. 3 shows the overall process of our approach. Then with the original ground-truth label, we will formulate $J + 1$ target trajectories as follows:

$$\tau_{conf} = \{c_0, c_1, \dots, c_J\}, \quad (6)$$

$$\tau_{tgt}^j = \{(x_1^{tgt_j}, y_1^{tgt_j}), (x_2^{tgt_j}, y_2^{tgt_j}), \dots, (x_T^{tgt_j}, y_T^{tgt_j})\}, \quad (7)$$

where τ_{tgt}^j is the j -th trajectory with score c^j , among $J + 1$ target trajectories. To simplify the notation, τ_{tgt}^0 is the ground-truth trajectory with c_0 set to 1.

Pseudo-Target Matching: Since we have a set of future trajectories and predictions for each target agent, the matching between future trajectories and ground-truth labels will be crucial. DETR [5] introduces the set predictor and utilizes Hungarian matching to pair the set of predictions and ground-truth labels. Instead of performing Hungarian matching, a naive approach can take the WTA strategy for each possible target. For each target, we find the predicted trajectory with the highest similarity as the source trajectory. The supervision will be enforced between the source and target trajectories.

3.4 Learning

The total supervision of our DCMS can be decoupled into several parts, as described in previous sections. For the regression and classification parts, we loop over all the possible $J + 1$ targets τ_{tgt} . For each target τ_{tgt}^j with confidence τ_{conf}^j , we apply WTA strategy as described in Sec. 3.3. Suppose k^* -th trajectory from trajectory refinement output τ_{reg}' is the best trajectory which has the maximum similarity with target τ_{tgt}^j , the classification loss and regression loss are defined as:

$$\mathcal{L}_{cls}^j = \frac{1}{K} \sum_{k=1}^K \tau_{conf}^j \mathcal{L}_{Huber}(c^k, c^{k^*}), \quad (8)$$

$$\mathcal{L}_{reg}^j = \frac{1}{T} \sum_{t=1}^T \tau_{conf}^j \mathcal{L}_{Huber}((x_t^{k^*}, y_t^{k^*}), (x_t^{tgt_j}, y_t^{tgt_j})). \quad (9)$$

For classification loss design, we adopt the displacement prediction idea from TPCN [51] to alleviate the hard assignment phenomenon. As for converting the displacement into probability, we use the standard softmax function to distribute the scores.

Since we have trajectory completion and refinement modules, the regression loss will be $\mathcal{L}_{reg} = \sum_{j=0}^J (\mathcal{L}_{reg}^j + \mathcal{L}_{\Delta reg}^j)$, where $\mathcal{L}_{\Delta reg}^j$ is the regression loss for the refinement module. The final loss consists of three parts: $\mathcal{L} = \mathcal{L}_{reg} + \mathcal{L}_{cls} + \mathcal{L}_{cons}$.

4 Experiments

We conduct experiments on the Argoverse dataset [8], one of the largest publicly available motion forecasting datasets. We first compare our DCMS with other state-of-the-art methods, and experiments show significant improvements in the evaluation metrics. Then we show the impact of dual consistency constraints on predicted trajectories with some qualitative results. Furthermore, we provide ablation studies to evaluate the effectiveness of each proposed module. Meanwhile, we design experiments for some hyperparameter choices. Finally, we extend our proposed modules to other methods to demonstrate their generalization ability.

4.1 Experimental Setup

Dataset: Argoverse [8] is currently one of the most popular motion forecasting datasets. It provides more than 300K scenarios with rich HDMap information. For each scenario, objects are divided into three types: agent, AV and others, respectively. And the object tagged with “agent” is the object to be predicted. Moreover, each scenario contains 50 frames sampled at 10Hz, meaning that the time interval between successive frames is 0.1s. Given the first 20 frames in the scenario as historical context, the task is to predict future trajectories for the “agent” objects for the next 30 frames. The whole datasets are split into training, validation, and test set, with 205942, 39472, and 78143 sequences, respectively.

Table 1. The detailed results of our DCMS and other top-performing approaches on the Argoverse test set. And b-FDE₆ is the abbreviation of brier-minFDE₆

| Models | minADE ₁ | minFDE ₁ | MR ₁ | minADE ₆ | minFDE ₆ | MR ₆ | b-FDE ₆ |
|-----------------------|---------------------|---------------------|-----------------|---------------------|---------------------|-----------------|--------------------|
| Jean [8,32] | 1.74 | 4.24 | 0.68 | 0.98 | 1.42 | 0.13 | 2.12 |
| LaneConv [27] | 1.71 | 3.78 | 0.59 | 0.87 | 1.36 | 0.16 | 2.05 |
| LaneRCNN [53] | 1.68 | 3.69 | 0.57 | 0.90 | 1.45 | 0.12 | 2.15 |
| mmTransformer [28] | 1.77 | 4.00 | 0.62 | 0.87 | 1.34 | 0.15 | 2.03 |
| SceneTransformer [34] | 1.81 | 4.06 | 0.59 | 0.80 | 1.23 | 0.126 | 1.88 |
| TNT [55] | 1.77 | 3.91 | 0.59 | 0.94 | 1.54 | 0.13 | 2.14 |
| DenseTNT [16] | 1.68 | 3.63 | 0.58 | 0.88 | 1.28 | 0.125 | 1.97 |
| PRIME [43] | 1.91 | 3.82 | 0.59 | 1.22 | 1.55 | 0.12 | 2.09 |
| TPCN [51] | 1.58 | 3.49 | 0.56 | 0.88 | 1.24 | 0.13 | 1.92 |
| HOME [15] | 1.70 | 3.68 | 0.57 | 0.89 | 1.29 | 0.08 | 1.86 |
| MultiPath++ [47] | 1.623 | 3.614 | 0.564 | 0.790 | 1.214 | 0.13 | 1.793 |
| Ours | 1.476 | 3.251 | 0.532 | 0.766 | 1.135 | 0.11 | 1.756 |

The test set only provides the first 2 seconds trajectories, with the ground-truth labels hidden. Furthermore, the map information which consists of lane points or polygons can be constructed by the given map API.

Metrics: We use the standard evaluation metrics, including ADE and FDE. ADE is defined as the average displacement error between ground-truth trajectories and predicted trajectories over all time steps. FDE is defined as displacement error between ground-truth trajectories and predicted trajectories at the last time step. We compute K likely trajectories for each scenario with the ground truth label. Therefore, minADE and minFDE are minimum ADE and FDE over the top K predictions. Moreover, miss rate (MR) is also considered, defined as the percentage of the best-predicted trajectories whose FDE is within a threshold (2m). Brier-minFDE is the minFDE plus $(1 - p)^2$, where p is the corresponding trajectory probability. Metrics for $K = 1$ and $K = 6$ are used in our experiments. Note that Brier-minFDE₆ is the ranking metric.

Experimental Details: We apply some standard data augmentation, including random flipping with a probability 0.5 and global random scaling with the scaling ratio between [0.8, 1.25] during the training stage. Following previous works [12,27,51], the coordinate system for each scenario is to be centered at the location of the target agent at $t = 0$. The orientation between the agent locations at $t = 0$ and $t = -1$ is used as the positive x-axis. As for some model settings, the time shift s for the temporal consistency constraint is set to 1. We adopt $K = 6$ to generate 6 trajectories and use $J = 6$ pseudo targets for each scenario. Furthermore, we choose bidirectional-matching and backward-matching strategies for temporal consistency constraint and Multi-Pseudo-Target respectively. We train DCMS for 50 epochs using a batch size of 32 with Adam [22] optimizer with an initial learning rate of 0.001, which is decayed every 15 epochs in a ratio of 0.1.

4.2 Experimental Results

Argoverse Leaderboard Results: We provide detailed quantitative results of our DCMS on the Argoverse test set as well as other public state-of-the-art methods in Tab. 1. Compared with previous methods, our DCMS improves all the evaluation metrics except MR_6 by a large margin, setting a new state-of-the-art performance for motion forecasting tasks. Furthermore, since the proposed modules are all general training components, other models can also benefit greatly from these strategies. Before March 23rd, we achieve **1st** place on the leaderboard for all $K = 1$ evaluation metrics and outperform the other state-of-the-art approaches by a large margin. Meanwhile, we also rank **1st** place for the main ranking metric $brier\text{-}minFDE_6$.

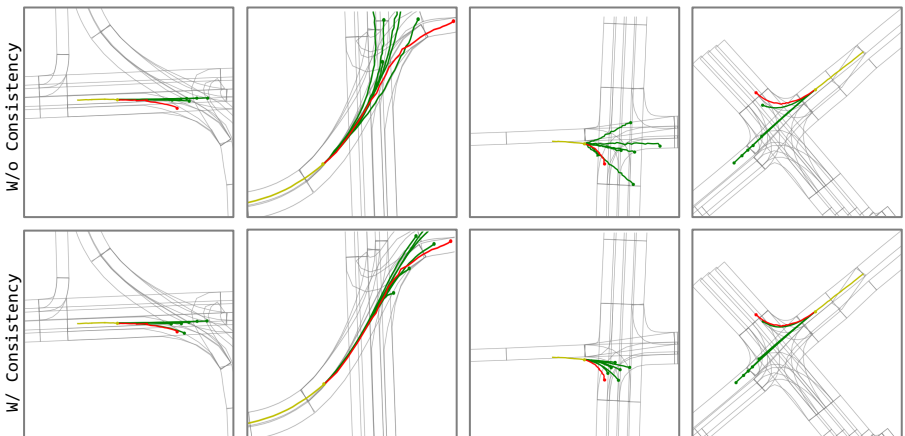


Fig. 4. The past trajectory is in yellow, the predicted trajectory in green, and the ground truth in red. The top row of the figure shows the results without consistency, while the bottom row shows the results with consistency

Qualitative Results: We also present some qualitative results on the Argoverse validation set in Fig. 4. Compared with results without consistency, the Dual Consistency Constraints improve both the quality and smoothness of the predicted trajectories significantly, resulting in more feasible and stable results despite the input noise.

4.3 Ablation Studies

Component Study: As shown in Tab. 2, we conduct an ablation study for our DCMS on the Argoverse validation set to evaluate the effectiveness of each proposed component. We adopt TPCN [51] as the baseline shown in the first row of Tab. 2 and add the proposed components progressively. The architecture modifications from goal set prediction and trajectory refinement module show

Table 2. Ablation study results of modules. Goal refers to Trajectory completion with goal prediction. “Ref.” is the trajectory refinement module, and the “Temp.” is temporal consistency. MPT refers to Multi-Pseudo-Target during training

| Architecture Goal | Consistency Ref. | Temp. | Spatial | MPT | K=1 | | K=6 | |
|----------------------|---------------------|-------|---------|-----|-------------|-------------|--------------|--------------|
| | | | | | minADE | minFDE | minADE | minFDE |
| | | | | | 1.34 | 2.95 | 0.73 | 1.15 |
| ✓ | | | | | 1.33 | 2.91 | 0.725 | 1.10 |
| ✓ | ✓ | | | | 1.31 | 2.89 | 0.71 | 1.07 |
| ✓ | ✓ | ✓ | | | 1.24 | 2.70 | 0.662 | 0.981 |
| ✓ | ✓ | ✓ | ✓ | | 1.22 | 2.67 | 0.653 | 0.954 |
| ✓ | ✓ | | | ✓ | 1.26 | 2.77 | 0.69 | 1.01 |
| ✓ | ✓ | ✓ | ✓ | ✓ | 1.19 | 2.60 | 0.640 | 0.929 |

Table 3. Ablation study on matching factor for temporal consistency. In this experiment, we remove the Multi-Pseudo-Target supervision to fairly study the effect

| Matching Strategy | Similarity | K=1 | | | K=6 | | |
|-------------------|------------|-------------|-------------|--------------|--------------|--------------|--------------|
| | | minADE | minFDE | MR | minADE | minFDE | MR |
| Forward | ADE | 1.25 | 2.70 | 0.46 | 0.670 | 0.982 | 0.089 |
| | FDE | 1.24 | 2.69 | 0.46 | 0.668 | 0.980 | 0.088 |
| Backward | ADE | 1.25 | 2.70 | 0.46 | 0.670 | 0.982 | 0.089 |
| | FDE | 1.24 | 2.68 | 0.46 | 0.667 | 0.958 | 0.085 |
| Bidirectional | ADE | 1.22 | 2.67 | 0.446 | 0.666 | 0.972 | 0.087 |
| | FDE | 1.22 | 2.67 | 0.445 | 0.653 | 0.954 | 0.084 |
| Hungarian | ADE | 1.24 | 2.69 | 0.46 | 0.668 | 0.975 | 0.088 |
| | FDE | 1.23 | 2.69 | 0.45 | 0.660 | 0.968 | 0.088 |

their promising improvements of about 2%. Dual consistency Constraints have the largest improvements of more than 5% among all the evaluation metrics. Especially for minFDE_1 , temporal consistency can optimize 20cm, indicating the temporal constraints can improve both final position and trajectory probability prediction. Compared with temporal consistency, spatial consistency has less effect on models since we only enforce this constraint in the trajectory refinement stage. Finally, the Multi-Pseudo-Target supervision significantly increases the performance, manifesting its effectiveness in helping training convergence.

Temporal Consistency Factors: Firstly, we study the factors in the matching problems, including similarity and matching strategies. As shown in Tab. 3, both Hungarian and Bidirectional matching show their advantages over the single direction matching. Although Hungarian matching can ensure the one-to-one matching relationship, it is sensitive to the similarity metric and numerical precision, both of which are not stable in the early training stage. In contrast, bidirectional matching with the FDE similarity metric nearly achieves the best results across all the evaluation metrics. Therefore, we choose bidirectional matching with the FDE similarity metric.

Table 4. Ablation study results of time-shift s used by temporal consistency

| Time shift s | K=1 | | | K=6 | | |
|-------------------|-------------|-------------|--------------|--------------|--------------|--------------|
| | minADE | minFDE | MR | minADE | minFDE | MR |
| 1 | 1.22 | 2.67 | 0.444 | 0.653 | 0.954 | 0.084 |
| 2 | 1.23 | 2.67 | 0.444 | 0.654 | 0.958 | 0.082 |
| 3 | 1.25 | 2.69 | 0.445 | 0.662 | 0.964 | 0.085 |
| 4 | 1.25 | 2.70 | 0.446 | 0.667 | 0.969 | 0.086 |

Table 5. Ablation study results on the pseudo target number J

| Pseudo Target Num J | K=1 | | | K=6 | | |
|--------------------------|-------------|-------------|-------------|-------------|-------------|-------------|
| | minADE | minFDE | MR | minADE | minFDE | MR |
| 1 | 1.29 | 2.82 | 0.50 | 0.70 | 1.03 | 0.104 |
| 3 | 1.28 | 2.80 | 0.48 | 0.69 | 1.02 | 0.10 |
| 6 | 1.26 | 2.77 | 0.47 | 0.69 | 1.01 | 0.09 |

Meanwhile, we also conduct experiments to find the best time-shift value s in the temporal consistency. As shown in Tab. 4, choosing time shift $s = 1$ has already achieved decent performance, with five out of six metrics ranking the first. Further increasing the s will not bring much performance gain since the driving behavior could change a lot with large s .

As shown in Tab. 5, more pseudo targets could bring better performance. Compared with $J = 1$, 6 pseudo targets bring an extra nearly 1% improvements. However, the marginal improvement decreases significantly so that we finally choose $J = 6$.

4.4 Generalization Capability

To verify the generalization capability of Dual Consistency Constraints and Multi-Pseudo-Target supervision, we also apply it to different models with state-of-the-art performance to show that they can be plugin-in training schemes.

Consistency Component: As shown in Tab. 6, our dual consistency constraints can effectively improve the performance of models regardless of their representations through the training phase. There is a noticeable improvement of over 5% on every metric, especially for minFDE.

Pseudo Target: Multi-Pseudo-Target is another general training trick that can be widely used in other frameworks. In Tab. 7, we also verify its effectiveness on other public methods. Methods with Multi-Pseudo-Target supervision have nearly over 3% improvement in all metrics. For the original DenseTNT [16], we replace its original handcrafted optimization for pseudo goal targets with our self-ensembling pseudo targets. This strategy brings an over 5% increase in performance, demonstrating the better quality of the self-ensembling pseudo targets than handcrafted optimizations and estimation.

Table 6. Ablation study of consistency constraints on different state-of-the-art methods on Argoverse validation set. Performance for methods without consistency constraints is obtained from corresponding papers or our reproduction

| Method | Consistency | K=1 | | K=6 | |
|--------------------|-------------|-------------|-------------|-------------|-------------|
| | | minADE | minFDE | minADE | minFDE |
| LaneGCN [27] | ✗ | 1.35 | 2.97 | 0.71 | 1.08 |
| | ✓ | 1.29 | 2.80 | 0.68 | 1.00 |
| TPCN [51] | ✗ | 1.34 | 2.95 | 0.73 | 1.15 |
| | ✓ | 1.27 | 2.79 | 0.69 | 1.04 |
| mmTransformer [28] | ✗ | 1.38 | 3.03 | 0.71 | 1.15 |
| | ✓ | 1.31 | 2.83 | 0.68 | 1.02 |
| DenseTNT [16] | ✗ | 1.36 | 2.94 | 0.73 | 1.05 |
| | ✓ | 1.25 | 2.81 | 0.68 | 0.98 |

Table 7. Ablation study of Multi-Pseudo-Target (MPT) supervision on different state-of-the-art models

| Method | MPT | K=1 | | K=6 | |
|--------------------|-----|-------------|-------------|-------------|-------------|
| | | minADE | minFDE | minADE | minFDE |
| LaneGCN [27] | ✗ | 1.35 | 2.97 | 0.71 | 1.08 |
| | ✓ | 1.30 | 2.88 | 0.69 | 1.04 |
| TPCN [51] | ✗ | 1.34 | 2.95 | 0.73 | 1.15 |
| | ✓ | 1.30 | 2.86 | 0.69 | 1.09 |
| mmTransformer [28] | ✗ | 1.38 | 3.03 | 0.71 | 1.15 |
| | ✓ | 1.29 | 2.80 | 0.68 | 1.04 |
| DenseTNT [16] | ✗ | 1.36 | 2.94 | 0.73 | 1.05 |
| | ✓ | 1.30 | 2.82 | 0.69 | 1.00 |

5 Limitations

Although the proposed method achieves state-of-the-art performance and can be universal components for motion forecasting tasks, it still has several drawbacks: 1). Our method lacks strong mathematical proof to support the proposed components; 2). It requires more training resources including GPUs to generate pseudo targets by self-ensembling. Meanwhile, when training is equipped with temporal consistency, the training time and memory usage will nearly double.

6 Conclusion

In this work, we propose DCMS, an effective architecture for the motion forecasting task to explicitly model the multi-modality. Based on the improved TPCN, we utilize the consistency regularization on both spatial and temporal domains to leverage the potential from the self-supervision, which is ignored by previous efforts. Besides that, we explicitly model the multi-modality by providing supervision with powerful self-ensembling techniques. Experimental results on the

Argoverse motion forecasting dataset show the effectiveness of our approach and generalization capability to other methods.

References

1. Bachman, P., Alsharif, O., Precup, D.: Learning with pseudo-ensembles. *Advances in neural information processing systems* **27**, 3365–3373 (2014)
2. Bansal, M., Krizhevsky, A., Ogale, A.: Chauffeurnet. In: *Robotics: Science and Systems XV* (2019)
3. Breuer, A., Le Xuan, Q., Termöhlen, J.A., Homoceanu, S., Fingscheidt, T.: Quo vadis? meaningful multiple trajectory hypotheses prediction in autonomous driving. In: *2021 IEEE International Intelligent Transportation Systems Conference (ITSC)*. pp. 637–644. IEEE (2021)
4. Cai, Z., Vasconcelos, N.: Cascade r-cnn: Delving into high quality object detection. In: *Proceedings of the IEEE conference on computer vision and pattern recognition*. pp. 6154–6162 (2018)
5. Carion, N., Massa, F., Synnaeve, G., Usunier, N., Kirillov, A., Zagoruyko, S.: End-to-end object detection with transformers. In: *European conference on computer vision*. pp. 213–229. Springer (2020)
6. Casas, S., Luo, W., Urtasun, R.: Intentnet: Learning to predict intention from raw sensor data. In: *Conference on Robot Learning*. pp. 947–956 (2018)
7. Chai, Y., Sapp, B., Bansal, M., Anguelov, D.: Multipath: Multiple probabilistic anchor trajectory hypotheses for behavior prediction. *arXiv preprint arXiv:1910.05449* (2019)
8. Chang, M.F., Lambert, J., Sangkloy, P., Singh, J., Bak, S., Hartnett, A., Wang, D., Carr, P., Lucey, S., Ramanan, D., et al.: Argoverse: 3d tracking and forecasting with rich maps. In: *Proceedings of the IEEE Conference on Computer Vision and Pattern Recognition*. pp. 8748–8757 (2019)
9. Dietterich, T.G.: Ensemble methods in machine learning. In: *International workshop on multiple classifier systems*. pp. 1–15. Springer (2000)
10. Duvenaud, D.K., Maclaurin, D., Iparraguirre, J., Bombarell, R., Hirzel, T., Aspuru-Guzik, A., Adams, R.P.: Convolutional networks on graphs for learning molecular fingerprints. In: *Advances in neural information processing systems*. pp. 2224–2232 (2015)
11. Fan, H., Zhu, F., Liu, C., Zhang, L., Zhuang, L., Li, D., Zhu, W., Hu, J., Li, H., Kong, Q.: Baidu apollo em motion planner. *arXiv preprint arXiv:1807.08048* (2018)
12. Fang, L., Jiang, Q., Shi, J., Zhou, B.: Tpnet: Trajectory proposal network for motion prediction. In: *Proceedings of the IEEE/CVF Conference on Computer Vision and Pattern Recognition*. pp. 6797–6806 (2020)
13. Földiák, P.: Learning invariance from transformation sequences. *Neural computation* **3**(2), 194–200 (1991)
14. Gao, J., Sun, C., Zhao, H., Shen, Y., Anguelov, D., Li, C., Schmid, C.: Vectornet: Encoding hd maps and agent dynamics from vectorized representation. In: *Proceedings of the IEEE/CVF Conference on Computer Vision and Pattern Recognition*. pp. 11525–11533 (2020)
15. Gilles, T., Sabatini, S., Tsishkou, D., Stanciulescu, B., Moutarde, F.: Home: Heatmap output for future motion estimation. *arXiv preprint arXiv:2105.10968* (2021)

16. Gu, J., Sun, C., Zhao, H.: Densetnt: End-to-end trajectory prediction from dense goal sets. In: Proceedings of the IEEE/CVF International Conference on Computer Vision. pp. 15303–15312 (2021)
17. Guzman-Rivera, A., Batra, D., Kohli, P.: Multiple choice learning: Learning to produce multiple structured outputs. Advances in neural information processing systems **25** (2012)
18. He, C., Zeng, H., Huang, J., Hua, X.S., Zhang, L.: Structure aware single-stage 3d object detection from point cloud. In: Proceedings of the IEEE/CVF Conference on Computer Vision and Pattern Recognition. pp. 11873–11882 (2020)
19. Henaff, M., Bruna, J., LeCun, Y.: Deep convolutional networks on graph-structured data. arXiv preprint arXiv:1506.05163 (2015)
20. Houenou, A., Bonnifait, P., Cherfaoui, V., Yao, W.: Vehicle trajectory prediction based on motion model and maneuver recognition. In: 2013 IEEE/RSJ international conference on intelligent robots and systems. pp. 4363–4369. IEEE (2013)
21. Kalman, R.E.: A new approach to linear filtering and prediction problems. J. Basic Eng **82**(1), 35–45 (1960)
22. Kingma, D.P., Ba, J.: Adam: A method for stochastic optimization. arXiv preprint arXiv:1412.6980 (2014)
23. Laine, S., Aila, T.: Temporal ensembling for semi-supervised learning. arXiv preprint arXiv:1610.02242 (2016)
24. Lee, D.H., et al.: Pseudo-label: The simple and efficient semi-supervised learning method for deep neural networks. In: Workshop on challenges in representation learning, ICML. vol. 3, p. 896 (2013)
25. Lee, S., Prakash, S.P.S., Cogswell, M., Ranjan, V., Crandall, D., Batra, D.: Stochastic multiple choice learning for training diverse deep ensembles. In: Advances in Neural Information Processing Systems. pp. 2119–2127 (2016)
26. Lei, C., Xing, Y., Chen, Q.: Blind video temporal consistency via deep video prior. Advances in Neural Information Processing Systems **33** (2020)
27. Liang, M., Yang, B., Hu, R., Chen, Y., Liao, R., Feng, S., Urtasun, R.: Learning lane graph representations for motion forecasting. In: Proceedings of the European Conference on Computer Vision (ECCV). pp. 541–556 (2020)
28. Liu, Y., Zhang, J., Fang, L., Jiang, Q., Zhou, B.: Multimodal motion prediction with stacked transformers. In: Proceedings of the IEEE/CVF Conference on Computer Vision and Pattern Recognition. pp. 7577–7586 (2021)
29. MacQueen, J., et al.: Some methods for classification and analysis of multivariate observations. In: Proceedings of the fifth Berkeley symposium on mathematical statistics and probability. vol. 1, pp. 281–297. Oakland, CA, USA (1967)
30. Makansi, O., Ilg, E., Cicek, O., Brox, T.: Overcoming limitations of mixture density networks: A sampling and fitting framework for multimodal future prediction. In: Proceedings of the IEEE/CVF Conference on Computer Vision and Pattern Recognition. pp. 7144–7153 (2019)
31. Mangalam, K., Girase, H., Agarwal, S., Lee, K.H., Adeli, E., Malik, J., Gaidon, A.: It is not the journey but the destination: Endpoint conditioned trajectory prediction. arXiv preprint arXiv:2004.02025 (2020)
32. Mercat, J., Gilles, T., El Zoghby, N., Sandou, G., Beauvois, D., Gil, G.P.: Multi-head attention for multi-modal joint vehicle motion forecasting. In: 2020 IEEE International Conference on Robotics and Automation (ICRA). pp. 9638–9644. IEEE (2020)
33. Narayanan, S., Moslemi, R., Pittaluga, F., Liu, B., Chandraker, M.: Divide-and-conquer for lane-aware diverse trajectory prediction. In: Proceedings of the

- IEEE/CVF Conference on Computer Vision and Pattern Recognition. pp. 15799–15808 (2021)
- 34. Ngiam, J., Caine, B., Vasudevan, V., Zhang, Z., Chiang, H.T.L., Ling, J., Roelofs, R., Bewley, A., Liu, C., Venugopal, A., et al.: Scene transformer: A unified multi-task model for behavior prediction and planning. arXiv preprint arXiv:2106.08417 (2021)
 - 35. Opitz, D., Maclin, R.: Popular ensemble methods: An empirical study. *Journal of artificial intelligence research* **11**, 169–198 (1999)
 - 36. Ouyang, H., Wang, T., Chen, Q.: Internal video inpainting by implicit long-range propagation. In: Proceedings of the IEEE/CVF International Conference on Computer Vision (ICCV). pp. 14579–14588 (October 2021)
 - 37. Phan-Minh, T., Grigore, E.C., Boulton, F.A., Beijbom, O., Wolff, E.M.: Covernet: Multimodal behavior prediction using trajectory sets. In: Proceedings of the IEEE/CVF Conference on Computer Vision and Pattern Recognition. pp. 14074–14083 (2020)
 - 38. Ren, S., He, K., Girshick, R., Sun, J.: Faster r-cnn: towards real-time object detection with region proposal networks. In: International Conference on Neural Information Processing Systems (2015)
 - 39. Rupprecht, C., Laina, I., DiPietro, R., Baust, M., Tombari, F., Navab, N., Hager, G.D.: Learning in an uncertain world: Representing ambiguity through multiple hypotheses. In: Proceedings of the IEEE International Conference on Computer Vision. pp. 3591–3600 (2017)
 - 40. Sajjadi, M., Javanmardi, M., Tasdizen, T.: Regularization with stochastic transformations and perturbations for deep semi-supervised learning. *Advances in neural information processing systems* **29**, 1163–1171 (2016)
 - 41. Schulz, J., Hubmann, C., Löchner, J., Burschka, D.: Interaction-aware probabilistic behavior prediction in urban environments. In: 2018 IEEE/RSJ International Conference on Intelligent Robots and Systems (IROS). pp. 3999–4006. IEEE (2018)
 - 42. Shuman, D.I., Narang, S.K., Frossard, P., Ortega, A., Vandergheynst, P.: The emerging field of signal processing on graphs: Extending high-dimensional data analysis to networks and other irregular domains. *IEEE signal processing magazine* **30**(3), 83–98 (2013)
 - 43. Song, H., Luan, D., Ding, W., Wang, M.Y., Chen, Q.: Learning to predict vehicle trajectories with model-based planning. In: Conference on Robot Learning. pp. 1035–1045. PMLR (2021)
 - 44. Sriram, N., Kumar, G., Singh, A., Karthik, M.S., Saurav, S., Bhowrnick, B., Krishna, K.M.: A hierarchical network for diverse trajectory proposals. In: 2019 IEEE Intelligent Vehicles Symposium (IV). pp. 689–694. IEEE (2019)
 - 45. Sun, P., Kretzschmar, H., Dotiwalla, X., Chouard, A., Patnaik, V., Tsui, P., Guo, J., Zhou, Y., Chai, Y., Caine, B., et al.: Scalability in perception for autonomous driving: Waymo open dataset. In: Proceedings of the IEEE/CVF Conference on Computer Vision and Pattern Recognition. pp. 2446–2454 (2020)
 - 46. Tarvainen, A., Valpola, H.: Mean teachers are better role models: Weight-averaged consistency targets improve semi-supervised deep learning results. *Advances in neural information processing systems* **30** (2017)
 - 47. Varadarajan, B., Hefny, A., Srivastava, A., Refaat, K.S., Nayakanti, N., Cornman, A., Chen, K., Douillard, B., Lam, C.P., Anguelov, D., et al.: Multipath++: Efficient information fusion and trajectory aggregation for behavior prediction. arXiv preprint arXiv:2111.14973 (2021)

48. Wang, T., Xie, J., Sun, W., Yan, Q., Chen, Q.: Dual-camera super-resolution with aligned attention modules. In: Proceedings of the IEEE/CVF International Conference on Computer Vision (ICCV). pp. 2001–2010 (October 2021)
49. Wang, X., Jabri, A., Efros, A.A.: Learning correspondence from the cycle-consistency of time. In: Proceedings of the IEEE/CVF Conference on Computer Vision and Pattern Recognition. pp. 2566–2576 (2019)
50. Xie, G., Gao, H., Qian, L., Huang, B., Li, K., Wang, J.: Vehicle trajectory prediction by integrating physics-and maneuver-based approaches using interactive multiple models. *IEEE Transactions on Industrial Electronics* **65**(7), 5999–6008 (2017)
51. Ye, M., Cao, T., Chen, Q.: Tpcn: Temporal point cloud networks for motion forecasting. In: Proceedings of the IEEE/CVF Conference on Computer Vision and Pattern Recognition. pp. 11318–11327 (2021)
52. Yu, L., Wang, S., Li, X., Fu, C.W., Heng, P.A.: Uncertainty-aware self-ensembling model for semi-supervised 3d left atrium segmentation. In: International Conference on Medical Image Computing and Computer-Assisted Intervention. pp. 605–613. Springer (2019)
53. Zeng, W., Liang, M., Liao, R., Urtasun, R.: Lanercnn: Distributed representations for graph-centric motion forecasting. *arXiv preprint arXiv:2101.06653* (2021)
54. Zeng, W., Luo, W., Suo, S., Sadat, A., Yang, B., Casas, S., Urtasun, R.: End-to-end interpretable neural motion planner. In: Proceedings of the IEEE Conference on Computer Vision and Pattern Recognition. pp. 8660–8669 (2019)
55. Zhao, H., Gao, J., Lan, T., Sun, C., Sapp, B., Varadarajan, B., Shen, Y., Shen, Y., Chai, Y., Schmid, C., et al.: Tnt: Target-driven trajectory prediction. *arXiv preprint arXiv:2008.08294* (2020)
56. Zheng, W., Tang, W., Jiang, L., Fu, C.W.: Se-ssd: Self-ensembling single-stage object detector from point cloud. In: Proceedings of the IEEE/CVF Conference on Computer Vision and Pattern Recognition. pp. 14494–14503 (2021)
57. Zhou, T., Brown, M., Snavely, N., Lowe, D.G.: Unsupervised learning of depth and ego-motion from video. In: Proceedings of the IEEE conference on computer vision and pattern recognition. pp. 1851–1858 (2017)
58. Ziegler, J., Bender, P., Schreiber, M., Lategahn, H., Strauss, T., Stiller, C., Dang, T., Franke, U., Appenrodt, N., Keller, C.G., et al.: Making bertha drive—an autonomous journey on a historic route. *IEEE Intelligent transportation systems magazine* **6**(2), 8–20 (2014)